Morphological Approach for Template Matching

GERALD JEAN FRANCIS BANON
SERGIO DONIZETE FARIA

INPE/DPI – Instituto Nacional de Pesquisas Espaciais / Divisão de Processamento de Imagens
Caixa Postal 515
12201–970 – São José dos Campos, SP, Brazil
banon@dpi.inpe.br
faria@dpi.inpe.br

Abstract. In this work, a morphological representation of a template matching algorithm for gray–scale images is presented. The algorithm is the composition of the so–called template matching operator with the maximum gray–level location operator, which can be both expressed in terms of the following classes of mathematical morphology elementary operators: dilations, erosions and anti–dilations. Moreover, the algorithm is applied to remote sensing images.

Keywords: Image processing, mathematical morphology, template matching, remote sensing.

1 Introduction

The template matching problem consists of finding out in a *search image* the location of a *template* (pattern). In some applications, for example in image registration, this template is extracted from a *reference image*.

In literature, we can find many techniques to perform template matching (Ballard & Brown, 1982; Goshtasby, 1985; Li & Dubes, 1985; Lemmens, 1988). These techniques can be classified in three groups: area–based (Barnea & Silverman, 1972; Moik, 1980), feature–based (Medioni & Nevatia, 1984; Hannah, 1988; Toth & Schenk, 1992; Flusser & Suk, 1994) and structural (Bins, 1988; Ventura et al., 1990; Haala & Vosselman, 1992).

The classical technique, among the area–based ones, derives from the normed vector space theory (Luenberger, 1969). In this approach, the images or templates are seen as vectors.

When the Euclidian norm is used, we get the well known correlation method (Barnea & Silverman, 1972) and the best fit is defined in terms of maximal correlation between two vectors. In this approach, the correlation is a sum of products.

When the so called l_1 norm is used, Maragos (1988) showed that minimizing it is equivalent to maximizing a nonlinear correlation, a sum of minima, which he called morphological correlation.

Following the nonlinear approach, Ronse (1996) characterized the template extraction by three requirements: the so called "overcondensation", anti–extensivity and idempotence. It is shown that an operator having these properties is the composition of an inf–separable operator (Banon & Barrera, 1993) followed by a dilation.

Moreover, Khosravi and Schafer (1996) used the sum of a gray–scale erosion and a gray–scale anti–dilation (both vertically invariant) with the same structuring function to perform a template matching within a signal corrupted by Gaussian or impulsive noises.

Our main objective in this paper is to introduce a simple template matching algorithm based on area and defined within the framework of the lattice theory and, more specifically, the mathematical morphology. In our approach the correlation is a sum of intersections of thresholdings.

More precisely, we use some elementary morphological operators (dilations, erosions and anti–dilations) to construct a template matching algorithm. This is an important issue because it can unify the way we process images.

Different from Maragos, we do not assume the vector space structure and different from Ronse, we do not include a dilation for template reconstruction at the end of the matching procedure. Finally, different from Khosravi and Schafer we use pairs of erosion and anti–dilation with distinct structuring functions.

In Section 2, we recall some basic definitions from mathematical morphology. In Section 3, we present our template matching algorithm in terms of some elementary morphological operators and, finally, in Section 4 we show an application to remote sensing images.

2 Mathematical Morphology

Originally, mathematical morphology was developed in the context of image analysis (Serra, 1982). Nowadays, an important part of it belongs to the lattice theory (Serra, 1988; Heijmans & Ronse, 1990).

A lattice is a partially ordered set in which the supremum and the infimum of two elements exist (Birkhoff, 1967). We denote as $a \vee b$ and $a \wedge b$, respectively, the supremum and the infimum of two elements a and b in the

lattice. If the lattice is finite then it has a least and a greatest element that we denote, respectively, as o and i.

Let $(L_1, \leq)$ and $(L_2, \leq)$ be two *finite* lattices. Let ψ be a mapping from $(L_1, \leq)$ to $(L_2, \leq)$. We will call ψ an *operator.*

By definition,

ψ is a *dilation* iff
$\psi(a \vee b) = \psi(a) \vee \psi(b)$ and $\psi(o) = o$;
ψ is an *erosion* iff
$\psi(a \wedge b) = \psi(a) \wedge \psi(b)$ and $\psi(i) = i$;
ψ is an *anti–dilation* iff
$\psi(a \vee b) = \psi(a) \wedge \psi(b)$ and $\psi(o) = i$;
ψ is an *anti–erosion* iff
$\psi(a \wedge b) = \psi(a) \vee \psi(b)$ and $\psi(i) = o$;

for any a and b in L_1. For the general case of complete lattice see Serra (1988), Heijmans & Ronse (1990), Banon & Barrera (1993).

These operators are called elementary operators of the mathematical morphology because from them, it is possible to represent any operators from $(L_1, \leq)$ to $(L_2, \leq)$ (Banon & Barrera, 1991, 1993).

3 Template Matching Algorithm

Exact template matching is useless in most of the practical applications. For example, in remote sensing two images of the same scene at different times or from different sensors are almost never equal. A template matching algorithm must be based on inexact matching (Shapiro & Haralick, 1981; Bins, 1988; Lemmens, 1988). From the mathematical morphology point of view, inexact matching can be achieved by defining intervals around reference values and by testing if *all* the values of interest are falling into them. Nevertheless, the requirement that *all* the conditions are satisfied is not reasonable in practice, and what we suggest here is to look for the situations where a *maximum* number of conditions are satisfied.

The template matching algorithm proposed is shown in Figure 1. In this figure, f is the *reference image* and g the *search image*. The template matching algorithm is composed of several operators, one in each block. In order to present each of them, we are now introducing some mathematical notations.

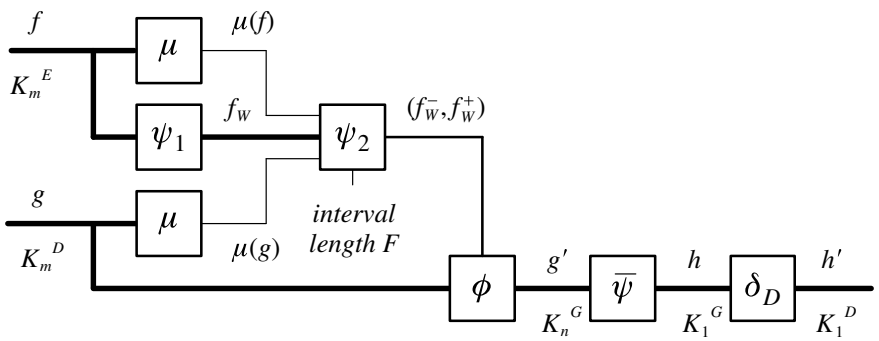

Fig. 1 – Template matching algorithm.

Let $\mathbf{Z}$ be the set of integer numbers, we denote as $\mathbf{Z}^2$ the Cartesian product $\mathbf{Z} \times \mathbf{Z}$. Let E be a finite rectangle of $\mathbf{Z}^2$, i.e., $E \triangleq I_1 \times I_2$, where I_1 and I_2 are two intervals of $\mathbf{Z}$; and let K_m be the interval $[0, m]$ of $\mathbf{Z}$. We denote the set of mappings from E to K_m as K_m^E. Actually, K_m^E represents the set of images with domain E and range K_m. In this work, we will need to deal with images having different domains, for this reason, we introduce one more finite rectangle of $\mathbf{Z}^2$ that we call D.

In Figure 1, the so–called measure μ is a mapping from E (or D) to $\mathbf{Z}$, defined by,

$$\mu(f) \triangleq \lfloor .5 + (1/\#E)\Big(\sum_{x \in E} f(x) \Big) \rfloor, \qquad (1)$$

for any f in K_m^E, where $\#E$ is the number of elements of E. Actually, $\mu(f)$ is an approximation of the average of the image f.

The template matching algorithm is aimed at searching for a given template f_W in the search image g. The template f_W is a subimage of f in the sense that W is a rectangle of $\mathbf{Z}^2$ called *window.*

In this section, for the sake of simplicity and without lose of generality we assume that W has a center (in other words, its number of rows and columns is odd) and this center is located at the origin of $\mathbf{Z}^2$, i.e., the point (0, 0).

The template f_W can be chosen manually or through an automatic procedure. In Figure 1, this procedure is represented by the operator ψ_1. In this work, we will not go into details about it.

The operator ψ_2 produces a pair of templates (f_W^-, f_W^+) from the template f_W in $K_m{}^W$. This pair of templates is defined in the following way:

$$f_W^-(x) \triangleq \max\{0,\ \min\{m,\ f_W(x) + c_1\}\} \quad (2)$$

$$f_W^+(x) \triangleq \max\{0,\ \min\{m,\ f_W(x) + c_2\}\} \quad (3)$$

for any x in W, where c_1 and c_2 ($c_1 \leq c_2$) are two integers depending on the averages $\mu(f)$ and $\mu(g)$, and a parameter F.

The two integers c_1 and c_2 are calculated in the following way:

$$c_1 = \mathrm{d}\mu - F/2 \quad \text{and} \quad c_2 = \mathrm{d}\mu + F/2 \quad (4)$$

where,

$$\mathrm{d}\mu = \mu(g) - \mu(f). \quad (5)$$

The parameter F defines the length of the interval $[c_1, c_2]$ centered at $d\mu$.

The parameter $d\mu$ is intended for reducing the image brightness difference. If f and g have the same average, then $d\mu$ is zero and no first order adjust is needed. Furthermore, we assume that both images have the same standard deviation, so no second order adjust is needed.

The search image g is looked over in order to find out the location of the best fit with the template f_W. This is done through the so called template matching operator ϕ (Figure 1). At this stage, we need to introduce some new notations.

Let G be the subset of $\mathbf{Z}^2$, given by $G = D \ominus W$, where the symbol $\ominus$ represents the Minkowski subtraction (Banon & Barrera, 1994), and let l be an integer number between 0 and m. The subset G, i.e., the difference of D and W, is a smaller rectangle compared to D, as shown in Figure 2. It will correspond to a reduce domain for further processed images.

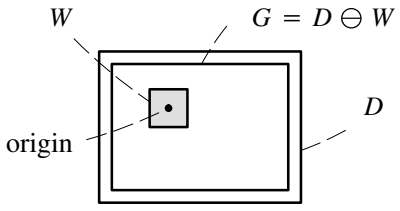

Fig. 2 – Domain reduction.

If n is the number of window elements, in other words $n = \#W$, then we denote as $\mathbf{n} \triangleq \{1, \ldots, n\}$ the set of integer numbers between 1 and n. For any integer number i in $\mathbf{n}$, we denote as $\varepsilon_l{}^i$ and $\delta_l{}^{ai}$ the operators from $K_m{}^D$ to $K_1{}^G$ defined by:

$$\varepsilon_l{}^i(g)(x) \triangleq \begin{cases} 1 & \text{if } g(x + w_i) \geq l \\ 0 & \text{otherwise} \end{cases} \quad (6a)$$

$$\delta_l{}^{ai}(g)(x) \triangleq \begin{cases} 1 & \text{if } g(x + w_i) \leq l \\ 0 & \text{otherwise} \end{cases} \quad (6b)$$

for any $g \in K_m{}^D$ and $x \in G$; where $i \mapsto w_i$ is a bijection from $\mathbf{n}$ to W, just for numbering the elements of W.

The pixel of the binary image $\varepsilon_l{}^i(g)$ (the transformed of $g \in K_m{}^D$ through $\varepsilon_l{}^i$), at position x has value 1 whenever the pixel of g at the neighborhood position $x + w_i$ has a value greater than or equal to l. For the operator $\delta_l{}^{ai}$, we just reverse the binary relation $\geq$.

By construction, the thresholding operators $\varepsilon_l{}^i$ and $\delta_l{}^{ai}$ are, respectively, erosions and anti–dilations from $(K_m{}^D, \leq)$ to $(K_1{}^G, \leq)$, where $\leq$ is the pointwise ordering derived from the ordering between gray–levels (Banon & Barrera, 1993; Faria, 1997).

We are now ready to introduce the template matching operator. We call *template matching operator* the operator ϕ from $K_m{}^D$ to $K_n{}^G$, given by:

$$\phi \triangleq \sum_{i \in \mathbf{n}} \lambda^i \quad (7)$$

where the λ^i's are n operators from $K_m{}^D$ to $K_1{}^G$, given by:

$$\lambda^i \triangleq \varepsilon^i_{f_W^-(w_i)} \wedge \delta^{ai}_{f_W^+(w_i)}. \quad (8)$$

Actually, the operators, like the λ^i's, which are the intersections of an erosion and an anti–dilation, are important in operator decomposition and are called *sup–generating operators* (Banon & Barrera, 1993). These operators for binary images are similar to the well known Hit–or–Miss operators (Serra, 1982).

Figure 3 shows the operator ϕ.

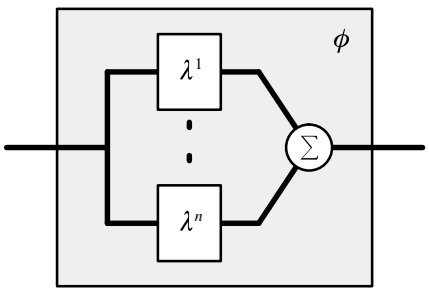

Fig. 3 – Template matching operator.

The pixel of the image $\lambda^i(g)$ (the transformed of $g \in K_m{}^D$ through λ^i), at position $x \in G$, has the value $\lambda^i(g)(x)$. This value is called the *matching condition*.

From Equations (6) and (7), the matching condition is 1 (i.e., satisfied) whenever $g(x + w_i)$ falls in the interval $[f_W^-(w_i), f_W^+(w_i)]$ and 0 (i.e., not satisfied) otherwise. Hence, we can see that $\phi(g)(x)$ simply indicates the number of satisfied conditions among n possible ones.

The operation of sum, appearing in the definition of ϕ, is an extension to operators of the sum of n numbers 0 or 1 which returns simply the number of 1's.

In other words, ϕ can be defined in an equivalent way by:

$$\phi(g)(x) = \#\{i \in \mathbf{n} : g(x + w_i) \in [f_W^-(w_i), f_W^+(w_i)]\},$$

for any $g \in {K_m}^D$ and $x \in G$. We can see that "behind" this expression we have a sum of n sup–generating operators.

Furthermore, we observe that the operator ϕ is the sum of intersections of thresholding operators.

In the next step, the image g' produced by ϕ is looked over through an operator $\overline{\psi}$ which locates its maximum pixel value and produces the image h (Figure 1). In order to present it we need to introduce some more notations.

For any integer number l between 0 and n, we denote as δ_l and ε_l the operators from ${K_n}^G$ to ${K_1}^G$ defined by:

$$\delta_l(f)(x) \triangleq \begin{cases} 1 & \text{if } f(x) > l \\ 0 & \text{otherwise} \end{cases}$$

$$\varepsilon_l(f)(x) \triangleq \begin{cases} 1 & \text{if } f(x) \geq l \\ 0 & \text{otherwise} \end{cases}$$

for any $f \in {K_n}^G$ and $x \in G$.

Like the operators of Equations (6), δ_l and ε_l are thresholding operators, but on the other hand, they are not neighborhood operators.

Furthermore, we denote as ${\delta_G}^{\mathrm{a}}$ the operator from ${K_1}^G$ to ${K_1}^G$ defined by:

$${\delta_G}^{\mathrm{a}}(f) \triangleq \begin{cases} 1_G & \text{if } f = 0_G \\ 0_G & \text{otherwise} \end{cases}$$

for any $f \in {K_1}^G$, where 0_G and 1_G are mappings from G to K_1 assuming, respectively, the constant values 0 and 1.

Finally, for any integer number l between 0 and n, we denote as ${\delta^{\mathrm{a}}}_l$ the operator from ${K_n}^G$ to ${K_1}^G$ defined by the composition:

$${\delta^{\mathrm{a}}}_l \triangleq {\delta_G}^{\mathrm{a}} \circ \delta_l.$$

By construction, the operators δ_l, ε_l and ${\delta^{\mathrm{a}}}_l$ are, respectively, dilations, erosions and anti–dilations from $({K_n}^G, \leq)$ to $({K_1}^G, \leq)$, and ${\delta_G}^{\mathrm{a}}$ is an anti–dilation from $({K_1}^G, \leq)$ to $({K_1}^G, \leq)$ (Banon & Barrera, 1993; Faria, 1997).

We are now ready to introduce the operator for maximum gray–level location. We call *maximum gray–level location operator* the operator $\overline{\psi}$ from ${K_n}^G$ to ${K_1}^G$, given by:

$$\overline{\psi} = \bigvee_{l\,=\,0,\,\ldots,\,n} \lambda_l \qquad (9)$$

where the λ_l's are $n + 1$ operators from ${K_n}^G$ to ${K_1}^G$, given by:

$$\lambda_l \triangleq \varepsilon_l \wedge {\delta^{\mathrm{a}}}_l.$$

For the same reason that we have seen above, the operators λ_l's are sup–generating operators. Figure 4 shows the operator $\overline{\psi}$.

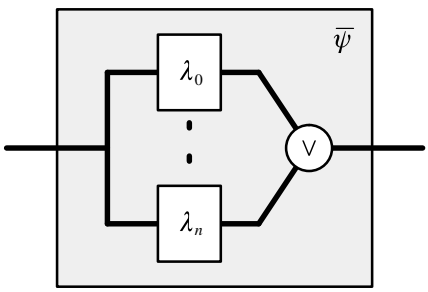

Fig. 4 – Maximum gray–level location operator.

The pixel of the binary image $\overline{\psi}(g')$ (the transformed of $g' \in {K_n}^G$ through $\overline{\psi}$), at position $x \in G$, has value 1 whenever the pixel of g' at this position has the greatest value among all the pixel values, i.e., has the value $\max g'(G)$.

In other words, $\overline{\psi}$ can be defined in an equivalent way by:

$$\overline{\psi}(g')(x) = \begin{cases} 1 & \text{if } g'(y) \leq g'(x) \quad (y \in G) \\ 0 & \text{otherwise} \end{cases},$$

for any $g' \in {K_n}^G$ e $x \in G$.

Actually, in the above representation of the operator for maximum gray–level location, there is an implicit thresholding decomposition of the input image (Banon, 1997).

The domain of the resulting image $h = \overline{\psi}(g')$ is G. In order to return to the original domain D of the search image, which is larger than G (actually, $D = G \oplus W$), we need one more step. Processing h through the last operator δ_D, we get the image h' showing where the template matching occurs in the proper domain of the search image (Figure 1). To achieve this expansion effect, while preserving the information contained in h, the operator δ_D from ${K_1}^G$ to ${K_1}^D$ must be define in this way:

$$\delta_D(h)(x) = \begin{cases} h(x) & \text{if } x \in G \\ 0 & \text{otherwise} \end{cases} \qquad (10)$$

for any $h \in K_1^G$ and $x \in D$. Furthermore, we observe that δ_D distributes over the union, i.e., it is a dilation from $(K_1^G, \leq)$ to $(K_1^D, \leq)$.

Figure 5 shows a numerical example where the images and the template are reduced to one–dimensional signals. In this example, w_2 coincides with the origin of $\mathbf{Z}^2$.

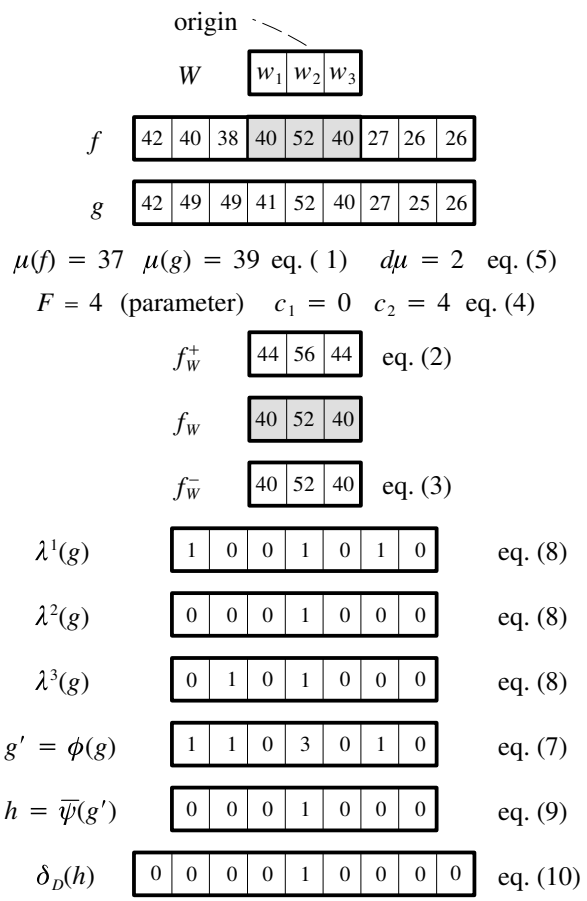

Fig. 5 – Numerical example.

4 Application to Remote Sensing Images

The template matching algorithm of Section 3 was used on remote sensing images (Faria, 1997). We present now the result of its application to a scene acquired from the Thematic Mapper (TM) sensor of the LANDSAT–5 satellite (path=220, row=77, quadrant=A, band=5), of a region near Itapeva in São Paulo State. We have used two TM subimages of size 360 by 360, one taken in September 09, 1990, as the reference image, and the other taken in July 18, 1994, as the search image.

In our experiment, we have chosen three different templates of size 51 × 51 in the reference image. The first column in Table 1 shows the position of the center of these templates. For each one, we have used three different values for the parameter *F*. For each of these values, Table 1 shows the maximum gray–level in $g'(G)$ and its position in the search image domain. The last column of Table 1 shows for each template its visual location obtained by a human operator.

TABLE 1 – EXPERIMENTAL RESULTS

Parameters of the Experiment		Result of the Algorithm		Visual Location
Template Center in the Reference Image *f* (col., row)	*F*	Maximum value in $g'(G)$	Position of the Maximum Value (col., row)	Template Location in the Search Image *g* (col., row)
(241,37)	15	580	(240,37)	(240,37)
	30	1151	(240,37)	
	45	1528	(240,37)	
(284,120)	15	571	(283,120)	(283,120)
	30	1057	(283,120)	
	45	1440	(283,120)	
(37,243)	15	657	(37,243)	(37,242)
	30	1250	(36,242)	
	45	1648	(36,242)	

In this experiment, the maximum gray–level in $g'(G)$ is unique. This is generally the case in remote sensing images. If it is not unique, some decision should be made depending on the final objective of the template matching.

Although the correct matching depends on the parameter *F*, we have observed that it can be achieved within a fairly large interval of values. For example, from Table 1, we observe that the result is not affected so much by a change in *F*.

Figure 6 shows the reference image *f* and the search image *g* used in the experiment. The small square in the domain of the reference image contains the second template of Table 1, i.e., the template of size 51 × 51 centered at position (284,120) as indicated by the small cross. The small square in the domain of the search image indicates the template visual location. Moreover, Figure 6 shows the images g' and h' obtained by running the algorithm with *F* equal to 15. The first one is a gray–level image which displays at each position the number of satisfied conditions in the matching process, and the last one is a binary image of one black point marking the place of the best matching.

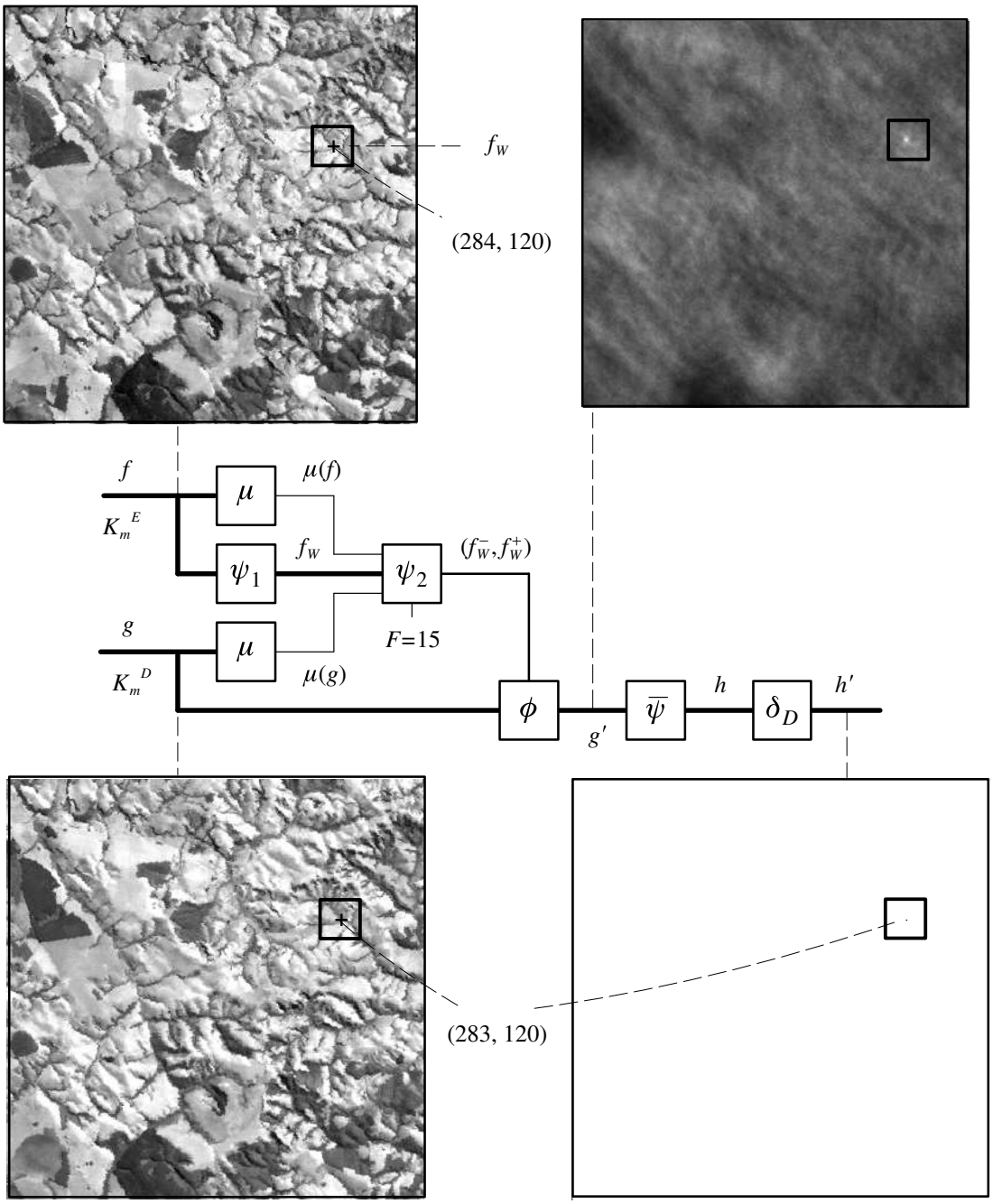

Fig. 6 – Application of the template matching algorithm to TM/LANDSAT images.

We observe that the output image g' of the template matching operator is very much like a correlation image, the brighter the pixel, the better the fit.

In this experiment, we see that the template matching algorithm was able to find out, in the search image, the right location of the template.

5 Conclusion

The template matching algorithm presented in this paper is the composition of three operators which have been defined in terms of dilations, erosions, and anti–dilations,

that is, in terms of some mathematical morphology elementary operators.

Different from other techniques, our template matching operator is the sum of intersections of thresholding operators.

The algorithm has been successfully applied to a pair of remote sensing images of the same scene. Three different templates from the reference images have been encountered at the right location in the search image.

In this way, we have shown that a simple template matching operator can be defined in terms of the elementary morphological operators.

Acknowledgment

During the period of this work, the authors have obtained support from CNPq (Conselho Nacional de Desenvolvimento Científico e Tecnológico) through the AnIMoMat project (contract 680067/94–9).

References

Ballard, D. H.; Brown, C. M. Matching. In: _____ *Computer vision*. New Jersey, Prentice Hall, 1982. cap. 11, p. 352–382.

Banon, G. J. F. Morphological decomposition of extreme gray–level location operators. In: Brazilian Workshop 97 on Mathematical Morphology, 1997, São José dos Campos, *Proceedings.*, Instituto Nacional de Pesquisas Espaciais, 1997. Available: <http://hermes.dpi.inpe.br:1905/rep/dpi.inpe.br/banon/1997/01.30.14.02>.

Banon, G. J. F.; Barrera, J. Minimal representations for translation–invariant set mappings by morphology mathematical. *SIAM Journal Applied Mathematic*, **51**(6):1782–1798, Dec. 1991.

Banon, G. J. F.; Barrera, J. Decomposition of mappings between complete lattices by mathematical morphology – part I: general lattices. *Signal Processing,* **30**(3):299–327, Feb. 1993.

Banon, G. J. F.; Barrera, J. *Bases da morfologia matemática para análise de imagens binárias.* IX Escola de Computação, Recife, julho de 1994. 248 p.

Barnea, D. I.; Silverman, H. F. A class of algorithms for fast digital image registration. *IEEE Transactions on Computers,* **21**(2):179–186, Feb. 1972.

Bins, L. S. *Uso do casamento estrutural para registro de imagens de satélite.* (Dissertação de Mestrado em Computação Aplicada) – Instituto Nacional de Pesquisas Espaciais, São José dos Campos, 1988. (INPE 4734–TDL/345).

Birkhoff, G. *Lattice theory.* 3.ed. Providence, Rhode Island, American Mathematical Society, 1967.

Faria, S. D. *Uma abordagem morfológica para casamento de padrões.* (Dissertação de Mestrado em Computação Aplicada) – Instituto Nacional de Pesquisas Espaciais, São José dos Campos, 1997. (INPE 6346–TDI/597). Available: <http://fenix.sid.inpe.br:1905/rep/dpi.inpe.br/faria/1997/04.16.15.30>.

Flusser, J.; Suk, T. A moment–based approach to registration of images with affine geometric distortion. *IEEE Transactions on Geoscience and Remote Sensing,* **32**(2):382–387, March 1994.

Goshtasby, A. Template matching in rotated images. *IEEE Transactions on Pattern Analysis and Machine Intelligence,* **7**(3):338–344, May 1985.

Haala, N; Vosselman, G. Recognition of road and river patterns by relational matching. In: International Archives of Photogrammetry and Remote Sensing, 17., Washington D. C., USA, 1992. Commission III, *Archives.*, Washington D. C., ISPRS, 1992. v.29, B3, p. 969–975.

Hannah, M. J. Digital stereo image matching techniques. In: International Archives of Photogrammetry and Remote Sensing, 16., Kyoto, Japan, 1988. Commission III, *Archives.*, Kyoto, ISPRS, 1988. v.27, B3, p. 280–293.

Heijmans, H. J. A. M; Ronse, C. The algebraic basis of mathematical morphology I: dilations and erosions. *Computer Vision, Graphics, & Image Processing,* **50**(3):245–295, 1990.

Khosravi, M.; Schafer, R. W. Template matching based on a grayscale hit–or–miss transform. *IEEE Transactions on Image Processing,* **5**(6):1060–1066, June 1996.

Lemmens, M. J. P. M. A survey on stereo matching techniques. In: International Archives of Photogrammetry and Remote Sensing, 16., Kyoto, Japan, 1988. Commission V, *Archives.*, Kyoto, ISPRS, 1988. v.27, B8, p. V.11–V.23.

Li, X.; Dubes, R. C. The first stage in two–stage template matching. *IEEE Transactions on Pattern Analysis and Machine Intelligence,* **7**(6):700–707, Nov. 1985.

Luenberger, D. G. *Optimization by vector space methods.* New York, John Willey & Sons, 1969. 326 p.

Maragos, P. Optimal morphological approaches to image matching and object detection. In: International Conference on Computer Vision, 2., 1988, p. 695–699.

Medioni, G.; Nevatia, R. Matching images using linear features. *IEEE Transactions on Pattern Analysis and Machine Intelligence,* **6**(6):675–685, Nov. 1984.

Moik, J. G. *Digital processing of remotely sensed images.* Washington, DC, NASA, 1980. 330 p.

Ronse, C. A lattice–theoretical morphological view on template extraction in images. *Journal of Visual Communication and Image Representation*, **7** (3):273–295, Sept. 1996.

Shapiro, L. G.; Haralick, R. M. Structural descriptions and inexact matching. *IEEE Transactions on Pattern Analysis and Machine Intelligence,* **3**(5):504–519, Sept. 1981.

Serra, J. *Image analysis and mathematical morphology.* London, Academic Press, 1982.

Serra, J. *Image analysis and mathematical morphology.* London, Academic Press, 1988. 2 v.

Toth, C. K.; Schenk, T. Feature–based matching for automatic image registration. *ITC Journal***, 1**:40–46, 1992.

Ventura, A. D.; Rampini, A.; Schettini, R. Image registration by recognition of corresponding structures. *IEE Transactions on Geoscience and Remote Sensing,* **28**(3):305–314, May 1990.